THE JOURNAL OF BIOLOGICAL CHEMISTRY VOL. 291, NO. 41, pp. 21644–21655, October 7, 2016

C4b-binding Protein Protects β-Cells from Islet Amyloid Polypeptide-induced Cytotoxicity*

Received for publication, April 5, 2016, and in revised form, August 15, 2016 Published, JBC Papers in Press, August 26, 2016, DOI 10.1074/jbc.M116.731141

Jonatan Sjölander[‡], Elin Byman[‡], Klaudia Kulak[‡], Sara C. Nilsson[‡], Enming Zhang[§], Ulrika Krus[§], Gunilla T. Westermark[¶], Petter Storm[§], Ben C. King[‡], Erik Renström[§], and Anna M. Blom[‡1]

From the Departments of [‡]Translational Medicine and [§]Clinical Sciences, Lund University, S-20502 Malmö, Sweden and the [¶]Department of Medical Cell Biology, Uppsala University, S-75123 Uppsala, Sweden

C4BP (C4b-binding protein) is a polymer of seven identical α chains and one unique β chain synthesized in liver and pancreas. We showed previously that C4BP enhances islet amyloid polypeptide (IAPP) fibril formation *in vitro*. Now we report that polymeric C4BP strongly inhibited lysis of human erythrocytes incubated with monomeric IAPP, whereas no lysis was observed after incubation with preformed IAPP fibrils. In contrast, incubation with the monomeric α-chain of C4BP was less effective. These data indicate that polymeric C4BP with multiple binding sites for IAPP neutralizes lytic activity of IAPP. Furthermore, addition of monomeric IAPP to a rat insulinoma cell line (INS-1) resulted in decreased cell viability, which was restored in the presence of physiological concentrations of C4BP. Treatment of INS-1 cells and primary rat islets with IAPP also diminished their ability to secrete insulin upon stimulation with glucose, which was reversed in the presence of C4BP. Further, C4BP was internalized together with IAPP into INS-1 cells. Pathway analyses of mRNA expression microarray data indicated that cells exposed to C4BP and IAPP in comparison with IAPP alone increased expression of genes involved in cholesterol synthesis. Depletion of cholesterol through methyl-β-cyclodextrin or cholesterol oxidase abolished the protective effect of C4BP on IAPP cytotoxicity of INS-1 cells. Also, inhibition of phosphoinositide 3-kinase but not NF-κB had a similar effect. Taken together, C4BP protects β-cells from IAPP cytotoxicity by modulating IAPP fibril formation extracellularly and also, after uptake by the cells, by enhancing cholesterol synthesis.

The present study focuses on C4BP[2] (C4b-binding protein), which is an essential inhibitor of the complement system (1). Complement has important roles in innate immunity and consists of more than 40 proteins involved in initiation and control of the system (2). C4BP is an abundant polymeric plasma protein that consists of seven identical α-chains with eight complement control protein (CCP) domains each, as well as one β-chain with three CCPs. The β-chain always carries anticoagulant PS (protein S) (3). Because of the high affinity of PS for negatively charged phospholipids, the C4BP-PS complex efficiently binds to apoptotic (4) and necrotic cells (5), ensuring controlled complement activation necessary for clearance of these cells. So far, C4BP has been characterized in detail as a complement inhibitor and is often employed by bacterial pathogens as a form of evasion strategy leading to decreased opsonization and phagocytosis (6). C4BP may have other immunomodulatory functions such as the induction of an anti-inflammatory state in dendritic cells (7). Complete deficiency of C4BP has not been described, but non-synonymous polymorphisms causing impaired complement inhibitory activity were found in atypical hemolytic uremic syndrome (8) and recurrent, spontaneous pregnancy loss (9). C4BP is mainly secreted by hepatocytes but significant expression is also detected in lung and pancreatic islets. We found previously that C4BP interacts with various types of amyloid (10–12), which similarly to in dying cells, allows a certain level of complement opsonization for clearance while preventing overt inflammation.

In type 2 diabetes amyloid deposits are localized to the islets of Langerhans in the pancreas and mainly formed by islet amyloid polypeptide (IAPP). IAPP deposits are present in 90% of patients with type 2 diabetes and can cause apoptosis of β-cells (13). Apart from this cytotoxic effect IAPP also has a physiological role in regulating and stabilizing blood glucose levels. When insulin resistance develops in type 2 diabetes, so does the production and release of insulin and concomitantly IAPP in the β-cell (14, 15). Once IAPP reaches a critical concentration, it starts to aggregate. The small aggregates form β-sheet-rich proto-filaments that interact with each other and eventually form mature fibrils. Even though the exact cytotoxic form of IAPP (monomers, oligomers, or fibrils) is still discussed, there is a growing consensus that small oligomers rather than the mature fibrils are responsible for the cytotoxic effect, similarly to Alzheimer's β-amyloid. It has also been suggested that it is the process of amyloid fibril formation in the membranes itself and not the presence of a particular IAPP species that is responsible for cytotoxicity (16, 17). We showed previously that C4BP enhances the kinetics of fibril formation (12), and we found C4BP to be co-localized with IAPP in human pancreatic islets, suggesting a beneficial role of C4BP in counteracting β-cell death in type 2 diabetes. Based on this hypothesis we now investigated the ability of C4BP to protect against IAPP-induced cytotoxicity in living cells and the molecular mechanism of this effect.

* This work was supported by the Knut and Alice Wallenberg Foundation and by Swedish Research Council Grants K2012-66X-14928-09-5. The authors declare that they have no conflicts of interest with the contents of this article.

[1] To whom correspondence should be addressed: Lund University, Dept. of Translational Medicine, Section of Medical Protein Chemistry, S-20502 Malmö, Sweden. Tel.: 46-40-338233; Fax: 46-40-337043; E-mail: anna.blom@med.lu.se.

[2] The abbreviations used are: C4BP, C4b-binding protein; CCP, complement control protein (domain); CHOD, cholesterol oxidase; DAF, decay accelerating factor; IAPP, islet amyloid polypeptide; MβCD, methyl-β-cyclodextrin; ANOVA, analysis of variance.

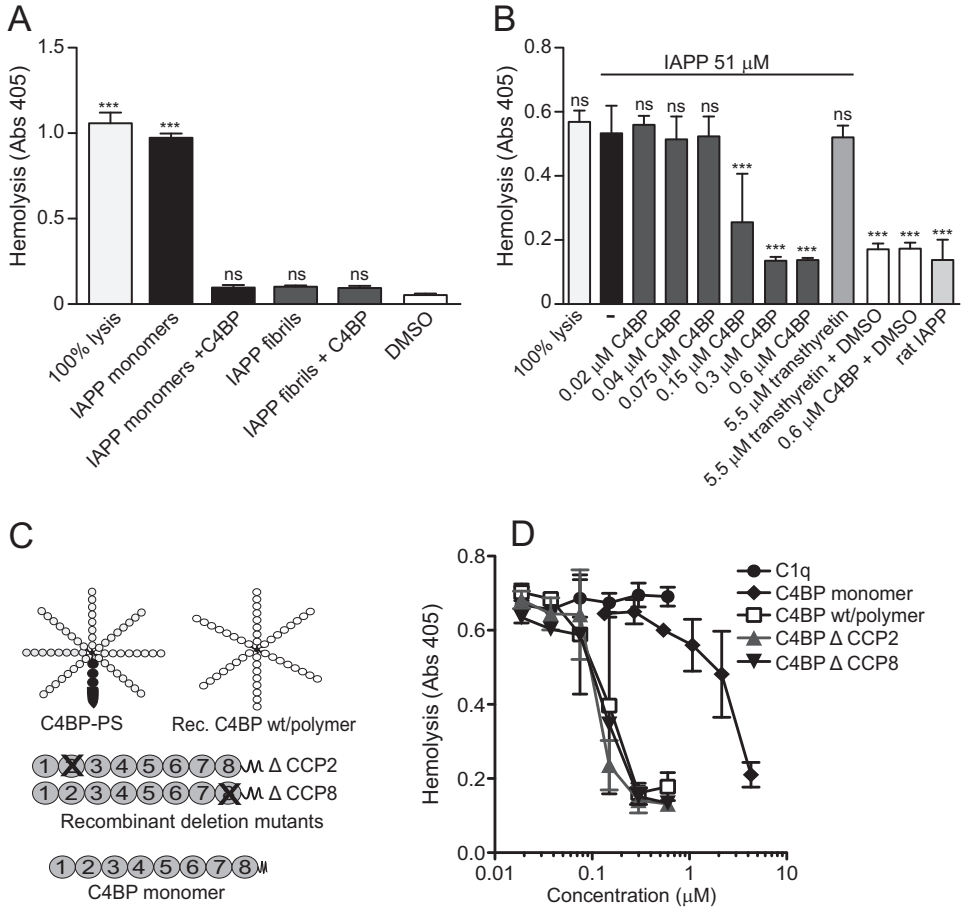

FIGURE 1. **Polymeric C4BP protects erythrocytes from lysis mediated by IAPP.** *A*, monomeric IAPP (51 μM) caused erythrocyte lysis in contrast to IAPP fibrils (51 μM) or 1% DMSO (vehicle). Addition of 0.6 μM C4BP together with 51 μM monomeric IAPP resulted in significant decreased in the lysis compared with monomeric IAPP alone. *B*, the inhibitory effect of C4BP on monomeric IAPP-induced erythrocyte lysis was concentration-dependent, whereas transthyretin showed no effect. Rat IAPP (51 μM) lacked the ability to lyse erythrocyte. *C*, a schematic illustration of the different C4BP variants used in this study. The prevalent form of C4BP found in plasma is composed of seven α-chains and one β-chain with bound PS. The recombinant C4BP lacks both β-chain and PS but retains the ability to bind amyloid. The panel also outlines the recombinant deletion mutants of C4BP that lack indicated CCP domains and a monomeric mutant, which consist of one α-chain that has a stop codon added after CCP8. *D*, all C4BP variants were added in various concentrations together with 51 μM monomeric IAPP. The monomeric C4BP was 20-fold less potent than wild type C4BP in inhibiting erythrocyte lysis, whereas mutants lacking CCP2 or CCP8 were comparable with the wild type. C1q, which also interacts with amyloid, was used as a control and did not affect monomeric IAPP-induced erythrocyte lysis. The graphs show mean values of three independent experiments $\pm$ S.D. One-way ANOVA with Dunnett's post-test was used for the statistical evaluation, and the various conditions were compared with DMSO alone (*A*) or monomeric human IAPP (*B*). *ns*, not significant; ***, $p < 0.001$.

Results

C4BP Protects Erythrocytes from Lysis Initiated by Monomeric IAPP—We hypothesized that because of the previously observed binding of IAPP, C4BP would have cytoprotective effect. Indeed, we found that the addition of IAPP fibrils (51 μM counted as monomer equivalents) to erythrocytes caused no significant cell lysis in comparison with 1% DMSO, which was present in all samples with IAPP (Fig. 1*A*), whereas addition of 51 μM monomeric IAPP to erythrocytes caused significant cell lysis (Fig. 1*A*) similar to maximal cell lysis obtained in water. Supplementing the monomeric IAPP solution (51 μM) with C4BP (0.6 μM) almost entirely abolished the lytic effect. Furthermore, addition of C4BP to the IAPP fibril solution had no effect on the already low degree of cell lysis (Fig. 1*A*). The effect was dependent on the concentration of C4BP (Fig. 1*B*), whereas transthyretin (5.5 μM) had no effect on lysis mediated by monomeric IAPP. Furthermore, we found that neither transthyretin alone (5.5 μM) nor C4BP alone (0.6 μM) had any effect on background erythrocyte lysis (Fig. 1*B*). We also verified that the observed effect of IAPP on erythrocyte lysis was specific for human IAPP because rat IAPP, which has not been observed to form oligomers and fibrils, caused no lysis (Fig. 1*B*).

Structural Requirements for Activity of C4BP—To further explore the mechanism whereby C4BP impairs IAPP-induced erythrocyte lysis, we utilized mutants of C4BP lacking either CCP2 or CCP8, which are the specific domains binding to IAPP (Fig. 1*C*) (12) and found that both mutants inhibited IAPP-mediated lysis at similar concentrations as wild type C4BP (Fig. 1*D*). We also tested a monomeric α-chain of C4BP and found that it was 20-fold less efficient in inhibiting monomeric IAPP-induced erythrocyte lysis as compared with wild type polymeric C4BP (Fig. 1*D*). Interestingly, C1q, which also binds IAPP (12) and has polymeric structure, did not affect IAPP-induced lysis.

C4BP Counteracts IAPP Cytotoxicity on INS-1 Cells—The cytoprotective effect of C4BP was then evaluated using a rat pancreatic β-cell line INS-1. To obtain a significant effect of IAPP on INS-1 cell viability, the cells were challenged with 102

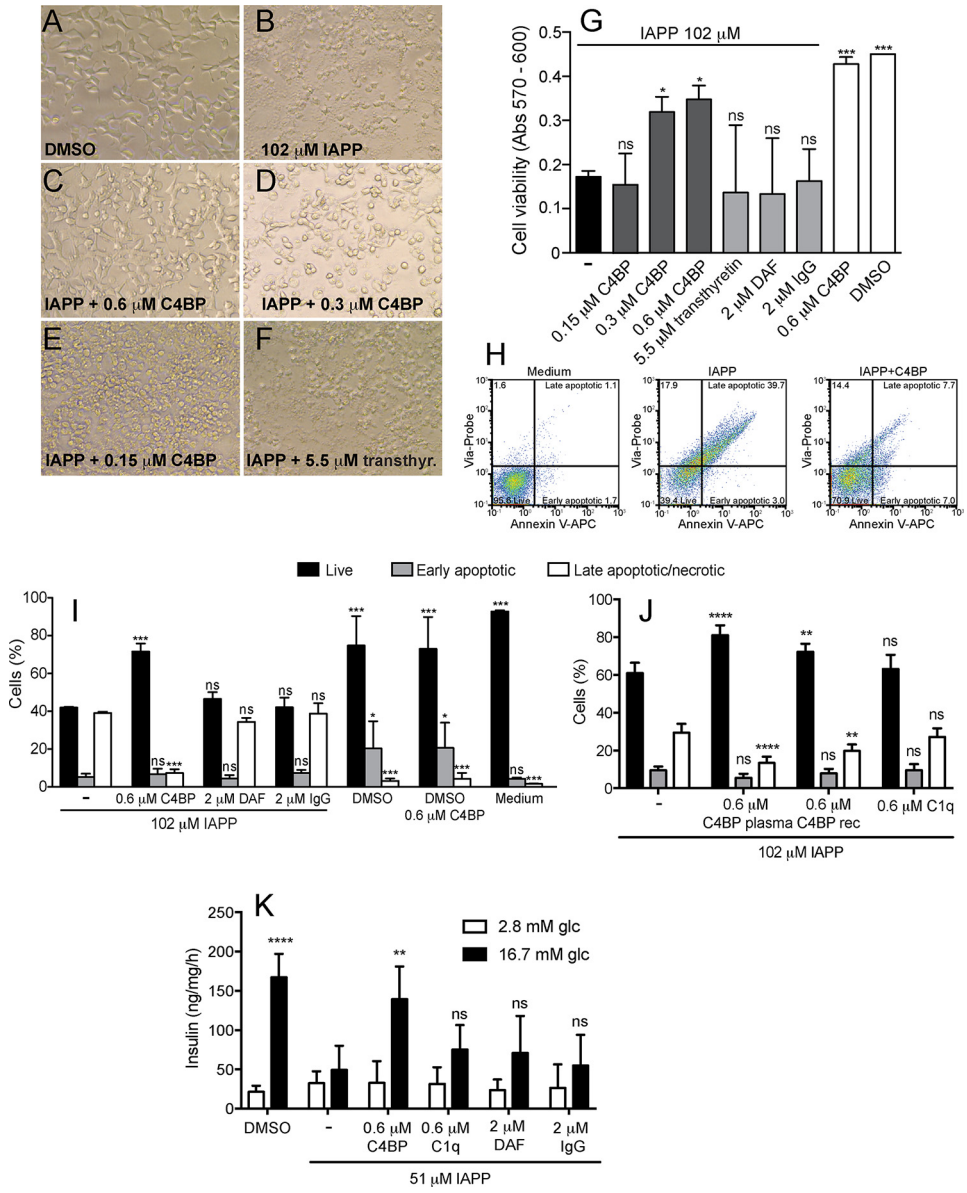

FIGURE 2. **C4BP increases viability of INS-1 cells incubated with IAPP.** *A–F*, INS-1 cells incubated 22 h in 1% DMSO (*A*), 102 μM monomeric IAPP alone (*B*) or together with 0.6 μM C4BP (*C*), 0.3 μM C4BP (*D*), 0.15 μM C4BP (*E*), or 5.5 μM transthyretin (*F*) are shown. The pictures were taken with an EVOS XL-core phase contrast microscope at 40× magnification. *G–J*, cell viability was quantitated using alamarBlue (*G*) or staining with Annexin V-APC and Via-Probe analyzed by flow cytometry (*H–J*). Dot plots (*H*) separate the stained cells into subgroups (live, early apoptotic, and late apoptotic/necrotic), and the percentage of the cells in each quadrant used for further calculations is shown. Cells incubated for 14 h with monomeric IAPP and C4BP (both purified from plasma and recombinant) had significantly higher viability then cells incubated with monomeric IAPP alone or together with either transthyretin, DAF, IgG, or C1q. *K*, cell death elicited by 51 μM IAPP was accompanied by failure of INS-1 cells to secrete insulin upon stimulation with glucose. The effect was prevented by addition of 0.6 μM C4BP but not control proteins C1q, DAF, and IgG. *G*, *I*, *J*, and *K* show mean values of three independent experiments performed in duplicate ± S.D. One-way ANOVA with Dunnett's post test (*G*) and two-way ANOVA with Bonferroni's post test (*I–K*) were used for the statistical evaluation, and various conditions were compared with IAPP alone. *ns*, not significant; *, $p < 0.05$; **, $p < 0.01$; ***, $p < 0.001$.

μM monomeric IAPP for 22 h. Under these conditions, cells exhibited an altered morphology, becoming more spherical (Fig. 2*B*) compared with the DMSO control (Fig. 2*A*). When 102 μM IAPP solution was supplemented with either 0.3 or 0.6 μM C4BP, the cells did not drastically change their morphology, compared with cells without IAPP (Fig. 2, *C* and *D*). However, when adding only 0.15 μM of C4BP together with 102 μM monomeric IAPP, the protective effect of C4BP was no longer present (Fig. 2*E*), and the morphological alteration was as prominent as for cells challenged with IAPP alone. Predominately spherical, dying cells were also observed in wells challenged with 102 μM IAPP in the presence of various control proteins such as DAF (2 μM, not shown), IgG (2 μM, not shown), or transthyretin (5.5 μM; Fig. 2*F*). Cell viability was then quantified using the alamarBlue® assay. The cells challenged with 102 μM monomeric IAPP alone had very low viability compared with cells exposed to co-solvent (DMSO) alone (Fig. 2*G*). Cells exposed to 102 μM monomeric IAPP in the presence of 0.3 or 0.6 μM C4BP were significantly more viable (Fig. 2*G*). Addition of 0.15 μM C4BP or any of the control proteins (2 μM DAF, 2 μM IgG, or 5.5 μM transthyretin) had no significant effect on IAPP-induced cell death.

Similar results were observed with cell viability measurements by flow cytometry after staining with Annexin V-APC and Via-Probe. The cells were gated into Annexin V and Via-Probe negative (live cells), Annexin V positive and Via-Probe negative (early apoptotic cells), and Annexin V and Via-Probe positive (late apoptotic cells) (Fig. 2*H*). Cells treated with only medium contained over 95% live cells (Fig. 2*H*, *left panel*), whereas the majority of cells treated with 102 μM monomeric IAPP bound both Annexin V and Via-Probe (Fig. 2*H*, *middle panel*). The cytotoxic effect of 102 μM IAPP was significantly reduced by the presence of 0.6 μM C4BP (Fig. 2, *H*, *right panel*; *I*; and *J*). INS-1 cells incubated with 102 μM IAPP and control proteins DAF (2 μM) and IgG (2 μM) did not show any increase in cell viability compared with IAPP alone. DMSO alone slightly decreased cell viability, and this effect was not attenuated by 0.6 μM C4BP, indicating that its protective effect is specific for IAPP-mediated cell death (Fig. 2*I*). Importantly, recombinant C4BP had a similar effect to that purified from plasma (Fig. 2*J*), whereas C1q, which also binds IAPP but does not enhance its polymerization, had no effect (Fig. 2*J*). Furthermore, INS-1 cells incubated with 51 μM IAPP did not respond with insulin secretion after incubation with 16.7 mM glucose (Fig. 2*K*). This functional defect was reverted in the presence of 0.6 μM C4BP but not control proteins: 0.6 μM C1q, 2 μM DAF, and 2 μM IgG.

C4BP Restores Insulin Secretion from Rat Islets Treated with IAPP—We first examined mRNA levels for *C4BPA* and *C4BPB* in isolated rat islets incubated in low and high glucose conditions. Although *C4BPB* expression remained stable under all conditions tested (Fig. 3*A*), *C4BPA* was highly up-regulated after 72 h of incubation. Glucose concentration did not affect expression of either of the genes. Further, we examine effect of IAPP on the ability of isolated rat islets to secrete insulin upon stimulation with 16.7 mM glucose. As expected, insulin secretion was impaired by incubation with 51 μM IAPP, likely because of decreased viability of the cells (Fig. 3*B*). This effect was largely rescued in the presence of 0.6 μM C4BP but not 0.6 μM C1q.

IAPP Alone and in Complex with C4BP Is Actively Internalized by INS-1 Cells—The protective effect of C4BP is likely in part because of its effect on fibril formation by IAPP. This should result in a decrease in cytotoxic oligomers, which otherwise are lytic for membranes. We further questioned whether C4BP may have additional intracellular effects. To investigate how IAPP alone or together with C4BP might interact with INS-1 cells, cells were treated with IAPP labeled with Rhodamine B and C4BP labeled with Alexa Fluor 647. IAPP (*blue*) and C4BP (*red*) together form large extracellular aggregates, some of which appeared to be localized to cell membranes (Fig. 4*A*). Complexes containing both IAPP and C4BP were also taken up into the INS-1 cells. We estimated that 52% of IAPP found intracellularly was in complexes with C4BP, whereas the remaining 48% was free (Fig. 4*C*). Cells treated with C4BP alone do not show any aggregates or intracellular staining (Fig. 4*B*). When IAPP (*blue*) was incubated with INS-1 cells in the presence or absence of C4BP followed by detection of mitochondria (*red*) and lysosomes (*green*), we observed that IAPP co-localizes

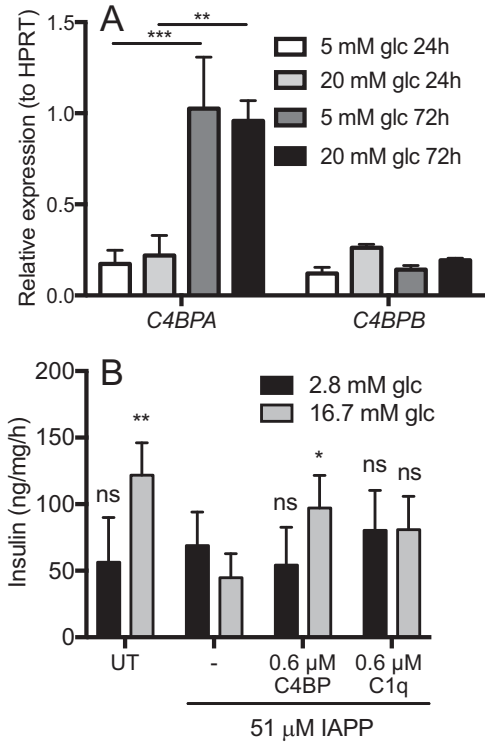

FIGURE 3. **C4BP rescues insulin secretion in primary rat islets treated with IAPP.** *A*, isolated rat islets were cultured *in vitro* for 24 or 72 h in either low (5 mM) or high (20 mM) glucose conditions. Expression of mRNA for *C4BPA* and *C4BPB* was measured in isolated mRNA by Q-PCR. Although *C4BPB* expression remained stable, *C4BPA* was highly increased during incubation albeit in glucose-independent manner. *B*, isolated rat islets were treated with 51 μM monomeric IAPP alone or together with 0.6 μM C4BP or 0.6 μM C1q overnight and thereafter stimulated with glucose to determine insulin secretion. IAPP impaired insulin secretion from rat islets, which was prevented by C4BP but not C1q. Shown are means ± S.D. from three independent experiments with sample duplicate, and statistical analysis was done with one-way ANOVA with Dunnett's post test, and the various conditions were compared with IAPP alone. *ns*, not significant; *UT*, untreated. *, $p < 0.05$; **, $p < 0.01$.

with both organelles (Fig. 4, *D* and *E*), and although there appears to be a tendency toward more IAPP present in cells in absence of C4BP (Fig. 4*G*), there did not seem to be any quantifiable difference in its distribution to the two organelles (Fig. 4*F*).

C4BP Modulates the Transcriptional Response to IAPP—Because C4BP is taken up by INS-1 cells together with IAPP, we hypothesized that it may affect cellular responses and mRNA expression levels of some targets, resulting in protection of cells from IAPP cytotoxicity. The global transcriptional response to 77 μM monomeric IAPP was therefore examined in INS-1 cells after 10 h of incubation in the presence or absence of 0.6 μM C4BP using the Affymetrix RaGene 2.0 array. Using linear models and empirical Bayesian moderation of *p* values, we identified 453 genes responding to IAPP in absence of C4BP (false discovery rate (FDR) *q* value < 0.05; Fig. 5*A*). Top scoring genes were among others JUN and DDIT3 coding for proteins jun proto-oncogene and DNA-damage inducible transcript 3, classical stress induced genes that were both up-regulated in response to IAPP. Gene ontology enrichment identified genes important for "response to organic substance," "regulation of programmed cell death," and "cellular lipid metabolism" as most

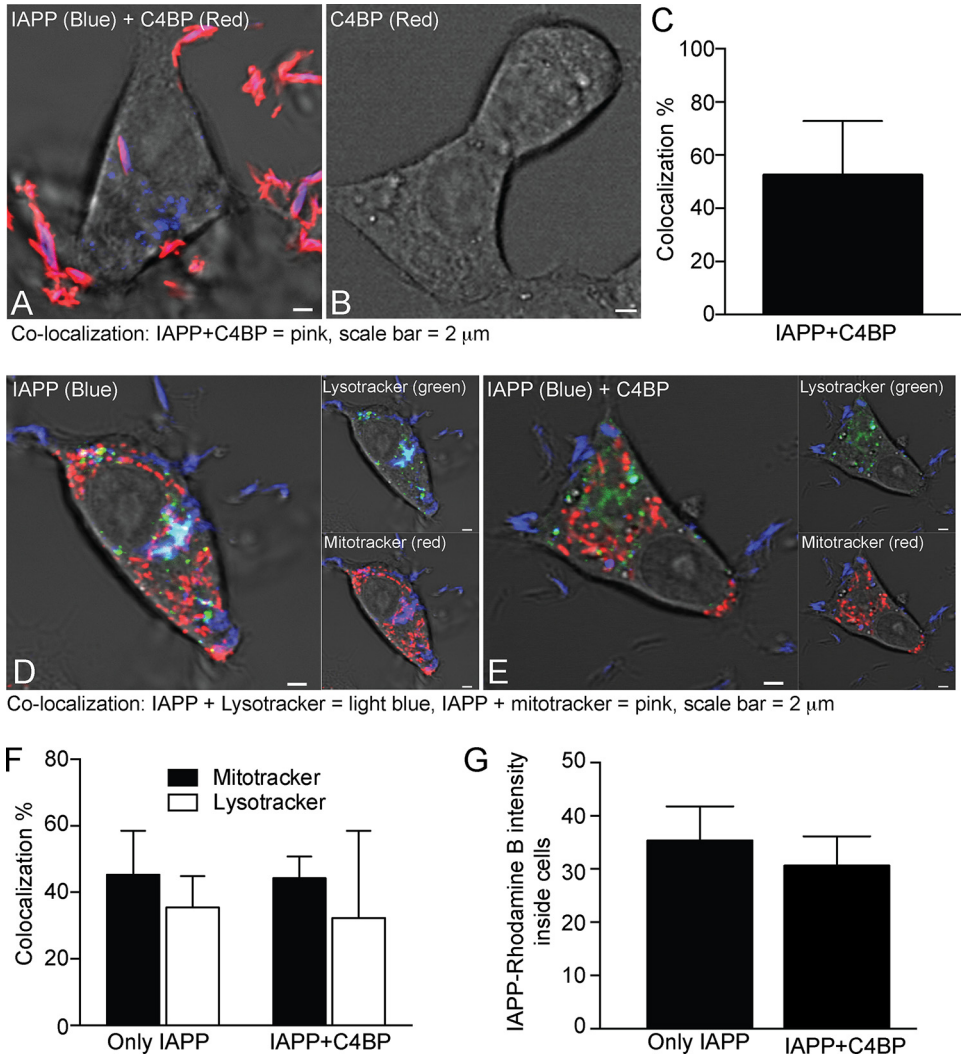

FIGURE 4. **C4BP and IAPP are internalized by INS-1 cells.** *A* and *B*, INS-1 cells incubated for 3 h with 51 μM Rhodamine B-labeled monomeric IAPP (*blue*) and 0.6 μM Alexa Fluor 647-labeled C4BP (*red*) (*A*) or 0.6 μM Alexa Fluor 647-labeled C4BP alone (*B*). *C*, IAPP and C4BP formed together large extracellular and intracellular aggregates leading to over 52% co-localization of IAPP with C4BP with 48% IAPP remaining free based on quantification of 12 individual cells, whereas no staining of INS-1 cells with C4BP alone was observed. *D* and *E*, INS-1 cells were also treated with 51 μM Rhodamine B-labeled monomeric IAPP without (*D*) and with 0.6 μM C4BP (*E*) together with LysoTracker Green and MitoTracker Deep Red for detection of lysosomes and mitochondria, respectively. *F* and *G*, co-localization of IAPP with mitochondria and lysosomes remained largely unchanged in the presence of C4BP (*F*), whereas there was a slight tendency toward decrease of IAPP inside the cells in the presence of C4BP (*G*). In *F* and *G*, means ± S.D. from three independent experiments in which at least 10 cells were quantified per condition are shown, and statistical analysis was done with two-way ANOVA with Bonferroni's post test (*F*) or *t* test (*G*) comparing conditions with and without C4BP. No statistically significant differences were observed.

affected, compatible with effects seen previously in IAPP treated cells (18–20).

Furthermore, 227 genes were found differentially expressed in response to IAPP in the presence of C4BP, of which 76 were identified also with IAPP alone and 151 were found to be regulated only in presence of both IAPP and C4BP. Sterol biosynthesis was the dominant Gene Ontology term in genes differentially expressed in the presence of C4BP (Fig. 5*B*; eight genes showed increased expression, $p < 10^{-6}$), suggesting that membrane remodeling might be an important mechanism underlying protective effect of C4BP in IAPP treated cells. Prominent genes up-regulated included *HMGCR* (coding for 3-hydroxy-3-methylglutaryl-CoA reductase, $p = 5.1 \times 10^{-5}$), the rate-limiting enzyme for cholesterol biosynthesis, and mevalonate (diphospho) decarboxylase that catalyzes mevalonate pyrophosphate into isopentenyl pyrophosphate in one of the early steps in cholesterol biosynthesis. Interestingly, enrichment of cell death-associated genes found in cells stimulated with IAPP alone was no longer observed in C4BP co-treated cells, indicating that the protective effect of C4BP occurs also on the transcriptional level. Ingenuity Pathway analysis confirmed the effects seen using Gene Ontology enrichment with "Superpathway of Cholesterol Biosynthesis" as the top scoring pathway ($p < 10^{-6}$).

Membrane-bound Cholesterol and Signaling through PI3K Pathway Are Important for the Protective Effect of C4BP—To verify the importance of cholesterol in the protective effect of C4BP, INS-1 cells were partially depleted from cholesterol using methyl-β-cyclodextrin (MβCD) or cholesterol oxidase (CHOD). The depleting effect of MβCD was confirmed by labeling of INS-1 cells with cholesterol binding molecule Filipin III (*green*) (Fig. 6, *A* and *B*). A similar effect was observed for CHOD-treated cells (Fig. 6*J*).

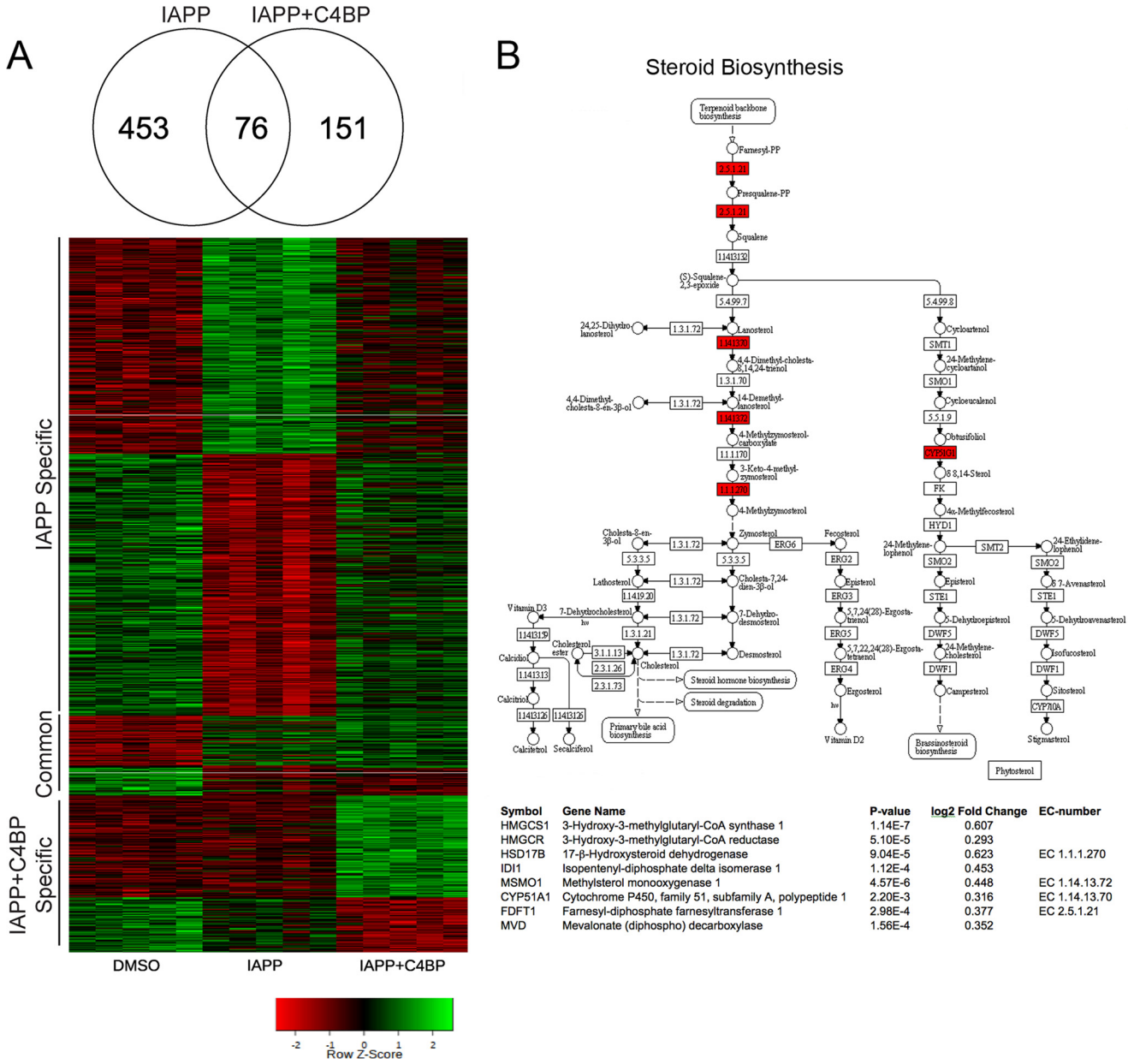

Symbol	Gene Name	P-value	log2 Fold Change	EC-number
HMGCS1	3-Hydroxy-3-methylglutaryl-CoA synthase 1	1.14E-7	0.607	
HMGCR	3-Hydroxy-3-methylglutaryl-CoA reductase	5.10E-5	0.293	
HSD17B	17-β-Hydroxysteroid dehydrogenase	9.04E-5	0.623	EC 1.1.1.270
IDI1	Isopentenyl-diphosphate delta isomerase 1	1.12E-4	0.453	
MSMO1	Methylsterol monooxygenase 1	4.57E-6	0.448	EC 1.14.13.72
CYP51A1	Cytochrome P450, family 51, subfamily A, polypeptide 1	2.20E-3	0.316	EC 1.14.13.70
FDFT1	Farnesyl-diphosphate farnesyltransferase 1	2.98E-4	0.377	EC 2.5.1.21
MVD	Mevalonate (diphospho) decarboxylase	1.56E-4	0.352	

FIGURE 5. **C4BP modulates transcription of cell death and cholesterol synthesis genes in response to IAPP.** *A*, analysis of mRNA expression in cells treated for 14 h with 77 μM IAPP alone or 77 μM IAPP together with 0.6 μM C4BP were performed using microarray analysis, and 680 genes were identified as differentially expressed (FDR-corrected $p < 0.05$) in any compared condition, 453 with IAPP alone, 76 in both IAPP, and IAPP + C4BP and 151 in only IAPP + C4BP. These genes were visualized in a heat map in which *red* denotes down-regulation (compared with DMSO control) and *green* represents up-regulation. *B*, representation of the Steroid Biosynthesis (KEGG00100) pathway with the genes identified as differentially expressed marked in *red* with full names, *p* values, and log2 fold changes (compared with untreated control) listed below.

The cell viability of INS-1 cells was then measured after depletion of cholesterol by MβCD and stimulation with 51 μM monomeric IAPP in the presence or absence of 0.3 μM C4BP. An increased binding of Annexin V was observed after incubation of INS-1 cells with IAPP (Fig. 6*D*), and this effect was diminished in the presence of C4BP as expected (Fig. 6*E*). Furthermore, the rescuing effect of C4BP was diminished when cells were preincubated with MβCD (Fig. 6, *H* and *I*). Cholesterol depletion with MβCD by itself did not affect cell viability in INS-1 cells (Fig. 5, *C* and *F*). Similar experiments were performed using CHOD to deplete cholesterol (Fig. 6, *J* and *K*), and there was a significantly higher ratio of Annexin V-positive apoptotic cells after IAPP + C4BP/IAPP treatment in CHOD-depleted cells compared with untreated cells with intact cholesterol content (Fig. 6*L*). These results indicate that membrane-bound cholesterol is important for the rescuing effect of C4BP in IAPP-treated cells.

To test the potential signaling pathways involved in the protective mechanism of C4BP, the INS-1 cells were treated with two signaling inhibitors, PI3K inhibitor (Ly29402 hydrochloride) and NF-κB inhibitor (BAY112085). Although the NF-κB inhibitor did not affect the ratio of apoptotic cells in IAPP + C4BP- *versus* IAPP-treated cells, the PI3K inhibitor significantly increased the number of apoptotic cells (Fig. 6*M*). This indicates that the protective effect of C4BP is at least in part elicited by signaling through the PI3K pathway.

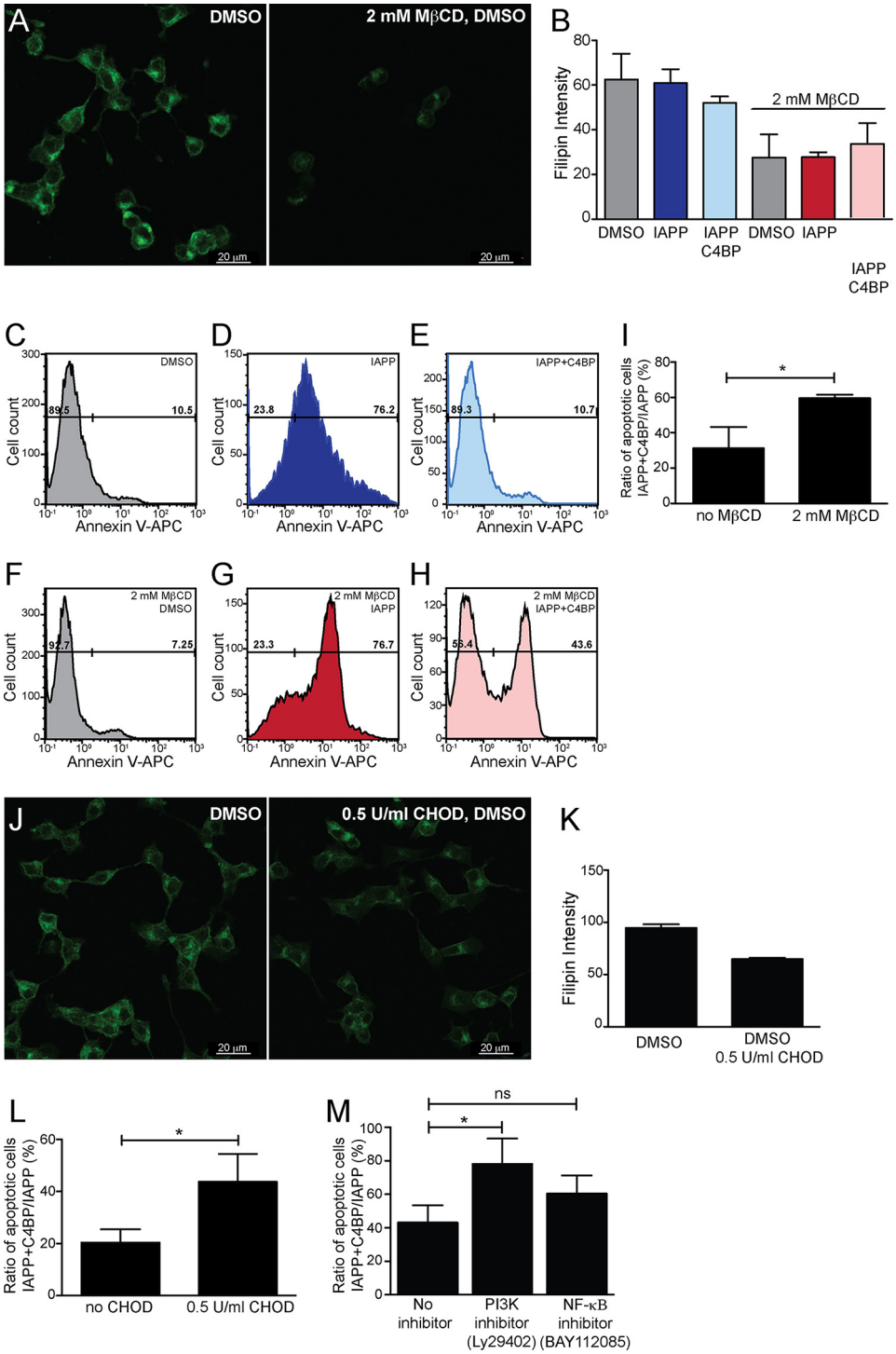

FIGURE 6. **Protective effect of C4BP requires cholesterol and signaling via PI3K pathways.** INS-1 cells were treated with cholesterol-depleting agent MβCD together with DMSO, 51 μM IAPP or 51 μM IAPP with 0.3 μM C4BP. *A*, INS-1 cells treated with either DMSO alone or together with MβCD and stained with Filipin III (*green*), indicating efficient depletion of cholesterol upon MβCD treatment. *B*, fluorescence intensity measurement of MβCD-treated and untreated INS-1 cells indicating depletion of cholesterol. The graph shows data from two independent experiments as means ± S.D. *C–H*, histograms showing INS-1 cells differing in cholesterol depletion with MβCD and treated with DMSO, 51 μM IAPP, or 51 μM IAPP with 0.3 μM C4BP for 14 h and stained with Annexin V-APC. The cells were gated into live (Annexin V-negative) and apoptotic (Annexin V-positive) populations. *I*, graph shows increase in the ratio of apoptotic cells between IAPP + C4BP-treated and IAPP-only-treated cells comparing cells treated with 2 mM MβCD with untreated controls. The data are from three independent experiments performed in duplicate and shown as means ± S.D. Statistical analysis was done with unpaired *t* test. *, $p < 0.05$. *J*, cholesterol was also depleted from INS-1 cells using a milder treatment with CHOD. *K*, the data showing decrease in Filipin III labeling intensity upon treatment with 0.5 unit/ml CHOD are from two independent experiments and shown as means ± S.D. *L*, an increase in the ratio of apoptotic cells between IAPP + C4BP-treated and IAPP-only-treated cells was observed in cells treated with 0.5 unit/ml CHOD compared with untreated controls. Shown are means ± S.D. from three independent experiments with sample duplicate, and statistical analysis was done with unpaired *t* test. *, $p < 0.05$). *M*, the ratio of apoptotic cells between treatments with 51 μM monomeric IAPP and 0.3 μM C4BP over 51 μM IAPP alone was increased in the presence of PI3K inhibitor (Ly29402) and not NF-κB inhibitor (BAY112085). Shown are means ± S.D. from three independent experiments with sample duplicate and statistical analysis was done with one-way ANOVA with Dunnett's post test and the various conditions were compared with no inhibitor. *, $p < 0.05$.

Discussion

C4BP was previously demonstrated to bind IAPP (12), and we now show that the presence of C4BP results in attenuation of cytotoxic effects of IAPP. Further, we identified several mechanisms underlying the protective effect of C4BP. First, by modulating fibrillation of IAPP, C4BP may cause a decrease in concentration of IAPP oligomers, which are otherwise able to cause lysis of eukaryotic cells such as erythrocytes. Further, C4BP also protects INS-1 cells from the cytotoxic effect of IAPP. This is likely in part due to lower oligomer concentration in the presence of C4BP. Furthermore, C4BP is also internalized by the INS-1 cells and affects their transcriptional activity. mRNA expression array analyses implicated that C4BP increased cholesterol synthesis, and the importance of cholesterol for the effect of C4BP was confirmed using two cholesterol-depleting reagents.

It is well established that incubation of human IAPP with cells results in formation of IAPP oligomers that are cytotoxic (21), which is at least in part mediated by direct cell membrane disruption by the oligomers, because the effect was also observed with cell-free lipid bilayers (22). We used human erythrocytes as a model to study membrane disruption during incubation with IAPP monomers. No lysis was observed when cells were incubated with IAPP fibrils, and the lytic effect of monomers was abolished in the presence of polymeric C4BP, which contains multiple binding sites for IAPP and thus is able to efficiently cross-link and co-aggregate with IAPP. We previously established that the binding site for IAPP is localized to CCP2 and CCP8 of C4BP, but polymeric mutants lacking one of these domains at a time had the same effect as wt C4BP. This can be explained by the fact that these mutants are still capable of multivalent interactions with IAPP (each mutant has six identical α-chains, each with one binding site for IAPP). Importantly, a C4BP monomer containing all domains except for the C-terminal polymerization fragment but having only two binding sites for IAPP (CCP2 and CCP8) largely lost protective activity. This indicates that the polymeric nature of C4BP containing multiple binding sites for IAPP (theoretically up to 12 simultaneous sites per one molecule of C4BP) is necessary for its protective effect. Interestingly, another large polymeric molecule that binds IAPP but does not cause increased fibril formation (12), C1q, showed no protective effect on erythrocyte lysis or INS-1 cell viability, indicating that the effect of C4BP is specific. One interesting aspect that requires further studies is that C4BP used in this study was purified from plasma and thus to a large degree is complexed with protein S, which is able to interact with negatively charged phospholipids such as phosphatidylserine. This ability of C4BP-protein S complex may be involved in its protective role because IAPP aggregation is enhanced in the presence of such lipids (23, 24). The C4BP-protein S complex may therefore interact with both phosphatidylserine and IAPP at the site of fibril formation. However, even recombinant wt C4BP, lacking the ability to bind protein S, had a cytoprotective effect when used in this study, showing that protein S is not necessary for the observed effect. It may, however, have modifying effects in the presence of phosphatidylserine, which will be studied in the future. Interestingly, C4BP has capacity to bind heparan sulfate (25, 26), and such proteoglycans on cell membrane are important for IAPP induced apoptosis (27).

Having established that C4BP-mediated enhanced fibril formation protected erythrocytes from direct lysis by IAPP, we also established that a β-cell line was similarly protected by C4BP from IAPP-mediated apoptosis. The effect of C4BP on cell survival was established using two independent methods, one relying on intact cell metabolism (alamarBlue) and the other measuring phosphatidyserine and DNA exposure (Annexin V and Via-Probe) using flow cytometry. In both methods, C4BP had a clear protective effect, whereas several control proteins, including DAF, another complement inhibitor composed of CCP domains, had no effect of IAPP cytotoxicity. The effect of C4BP is likely in part mediated by accelerated fibrillation of IAPP, and we indeed observed large extracellular aggregates composed of IAPP and C4BP both present extracellularly and also associated with cell membranes. We confirmed the cytoprotective effect of C4BP using primary rat islets treated with IAPP. Under such conditions, rat islets lost their ability to secrete insulin upon stimulation with glucose likely because of ongoing cell death. In the presence of C4BP, but not C1q, secretion was restored. Interestingly, cells treated with IAPP in the absence of C4BP had higher basal secretion of insulin, which is likely the result of ongoing apoptosis. Further, mRNA levels for *C4BPA* were highly up-regulated after 72 h of incubation of islets *in vitro*. Because C4BP is an acute phase protein, this finding is in agreement with observation that isolated islets show pro-inflammatory gene expression signature, which increases with time (28). In addition to being directly cytotoxic, IAPP induces inflammasome-dependent inflammation in the islet (29), and it is therefore likely that IAPP can therefore indirectly cause up-regulation of C4BP expression in the islet.

Furthermore, we found that INS-1 cells internalized certain amounts of IAPP, which then partially co-localized with both lysosomes and mitochondria. In the presence of C4BP, less IAPP appeared to be internalized, but it was clearly detectable in the cells, and 52% of intracellular IAPP was co-localized with C4BP. Our initial hypothesis was that perhaps there would be less co-localization of IAPP with mitochondria in the presence of C4BP, because such co-localization is related to apoptosis induction (30), but we failed to observe such a difference. We therefore queried whether IAPP affected transcriptional activity of the cell differently when internalized together with C4BP. Indeed, we found that treatment of INS-1 cells with IAPP alone caused up-regulation of pathways associated with apoptosis induction, whereas such an effect was not detected in cells treated with IAPP and C4BP. Instead we found up-regulation of several genes involved in cholesterol synthesis, leading to a hypothesis that C4BP rescues the cells partly via its effect on cholesterol synthesis.

To evaluate the role of cholesterol in the protective role of C4BP, we used two reagents that result in partial depletion of membrane cholesterol and disruption of lipid rafts. MβCD acts by forming soluble inclusions with cholesterol, rendering it soluble in aqueous environments (31). CHOD is a bacterial flavoenzyme that catalyzes the oxidation and isomerization of cholesterol (32). CHOD binds transiently to outer cell membranes, whereas leaving the intracellular cholesterol content

unchanged. As expected, we found that treatment of INS-1 cells with MβCD resulted in a larger decrease in cholesterol content measured by Filipin III staining as compared with CHOD. However, the protective effect of C4BP against IAPP insult was diminished upon treatment with any of the reagents, indicating that it is likely relying on the cholesterol content in the outer membrane. Direct contact of IAPP aggregates with cell membranes is needed to elicit apoptosis (18), which may proceed because of membrane destabilization and cation channel formation in cell membranes (17, 33). Cholesterol plays an important role in IAPP fibrillation and oligomer toxicity (34). Although IAPP fibrillation is enhanced by the presence of negatively charged phospholipids, addition of cholesterol to such anionic membranes had the opposite effect (35). Cholesterol regulates membrane fluidity and is found in lipid rafts, which include clusters of protein complexes. IAPP oligomers co-localize with the lipid raft marker, cholera toxin (20). Depletion of cholesterol by MβCD or statins is reported to inhibit internalization of IAPP oligomers via lipid raft-dependent endocytosis (20). This in turn enhanced extracellular oligomer accumulation and potentiated IAPP cytotoxicity. Furthermore, cholesterol depletion augmented the cytotoxic seeding capacity of IAPP oligomers across the plasma membrane (20). Our finding that the protective effect of C4BP appears to be related to an increase in cholesterol synthesis and abolished after cholesterol depletion is in good agreement with observations that cell susceptibility to IAPP insult is inversely related to plasma membrane cholesterol levels.

To gain insight into signaling pathways potentially involved in mediation of the protective effect of C4BP, we tested the effect of inhibitors of PI3K and NF-κB signaling pathways. The effect of C4BP was largely diminished in the presence of the PI3K pathway inhibitor, indicating involvement of the PI3K signaling pathway in the protective effect of C4BP. Interestingly, rosiglitazone, which is a ligand and activator of peroxisome proliferator-activated receptor γ and may be used to treat type 2 diabetes, also protects β-cells from IAPP toxicity and acts via activation of the PI3K pathway similarly to what we now observe for the protective effect of C4BP (36). Activation of the PI3K pathway leads to Akt phosphorylation, and consistently, overexpression of Akt in mouse β-cells increased their survival and improved glucose tolerance and resistance to experimental diabetes (37). The PI3K-Akt pathway is well known to play an important role in cell survival and protection from apoptosis. Taken together, these results lead to identification of a novel role for the complement inhibitor C4BP in the protection of β-cells from IAPP toxicity, which at least in part may explain the enigma of why this protein with very restricted expression pattern is expressed in pancreatic islets.

Experimental Procedures

Proteins—C4BP (38) and C1q (39) were purified from human plasma as described previously. C4BP was largely in complex with protein S. Recombinant C4BP wild type and mutants lacking either CCP 2 or CCP 8 domain as well the monomeric C4BP mutant consisting of eight CCP domains of the α-chain but lacking the C-terminal extension because of insertion of a premature STOP codon were expressed in eukaryotic cells and purified by affinity chromatography as described (40). C4BP was also labeled with Alexa Fluor 647 using Alexa Fluor 647 microscale protein labeling kit (Molecular Probes). Transthyretin purified from human plasma was a kind gift from late prof. Carl-Bertil Laurell. Human IgG was purchased from Immuno. Recombinant DAF with Fc tag was expressed and purified as described (41). IAPP was purchased from Caslo, Cambridge Research Biochemicals or synthesized and purified by Dr. James I. Elliott (Oxford, CT) and dissolved in DMSO at 20–40 mg/ml. Such stock was further diluted in assay buffers and used immediately to study IAPP monomers/oligomers. To obtain fibrils, IAPP was diluted in H_2O to 1 mg/ml and incubated for at least 7 days at room temperature. All three different preparations of IAPP yielded similar results, but we had to adjust exact concentrations of IAPP by titration for every new preparation, and these concentrations varied between 51 and 102 μM (200 and 400 μg/ml) to obtain similar cytotoxic effect. Concentrations of IAPP chosen for each type of experiment were based on initial titrations for every preparation of the peptide. Rat IAPP was from Bachem and dissolved in DMSO at 20 mg/ml.

Islet Isolation and Culture—Wistar male rats (Taconic) were used with ethical permit M205-07 (Lund University). Isolated pancreatic islets were prepared by collagenase P (Roche Applied Science) digestion and handpicked under a stereo microscope. For mRNA analysis, 100 islets/rat were cultured in RPMI 1640 tissue culture medium containing 5 or 20 mM glucose for either 24 or 72 h. The medium was supplemented with 10% FBS (Gibco), 100 units/ml streptomycin, and 100 units/ml penicillin (HyClone). Rat islets were also treated with 51 μM IAPP alone or supplemented with 0.6 μM C4BP or 0.6 μM C1q in Optimem (Gibco) overnight. For measurement of insulin secretion, freshly isolated islets were incubated in Krebs-Ringer buffer (10 mM HEPES, 1.2 mM KH_2PO_4, 120 mM NaCl, 4.7 mM KCl, 1.2 mM $MgSO_4$, 2.5 mM $CaCl_2$, 25 mM $NaHCO_3$, 0.1% BSA) supplemented with 2.8 or 16.7 mM glucose for 1 h. The secreted insulin was measured with ELISA detecting both rat and human insulin (Mercodia). Insulin release was normalized to total protein content determined using BCA Assay (Pierce).

RNA Isolation and Quantitative PCR—RNA was extracted from rat islets using RNAeasy kit (Qiagen). cDNA was produced by reverse transcription using oligo(dT) primers (Invitrogen), and then quantitative PCR was performed using TaqMan assays (Thermo Fisher Scientific) for rat *C4BPA*, *C4BPB* and reference gene hypoxanthine guanine phosphoribosyl transferase, using a ViiA7 real time PCR system (Thermo Fisher Scientific).

Hemolytic Amyloid Assay Testing IAPP-induced Lysis—Blood was drawn from healthy volunteers with approval of the ethics committee in Lund, and the erythrocytes were separated using Histopaque-1119. The isolated erythrocytes were washed in PBS until the supernatant was clear. The amount of erythrocytes added to each well in the 96-well plate (V-bottom; Nunc) was adjusted so that 100% lysis would yield an absorbance value of 0.7–1.3. To initiate cell lysis, PBC containing 51 μM monomeric IAPP or 51 μM IAPP fibrils was added alone or together with various concentrations of recombinant wild type or plasma purified C4BP, C1q, transthyretin, the monomeric α-chain of C4BP, C4BP ΔCCP8, and C4BP ΔCCP2. Because

diluted IAPP contained traces of DMSO, 1% DMSO alone was used as control. The erythrocytes were then incubated under these conditions for 2 h at 37 °C under gentle agitation. The experiment was terminated by a centrifugation at 800 × *g* for 5 min, after which the supernatants were transferred to a 96-well plate (Sterlin), and the absorbance of each well was determined at 405 nm in Carry 50 (Varian).

Cell Viability Assays—Rat insulinoma cells INS-1 832/13 cells (42) were grown in RPMI 1640 (HyClone) supplemented with 25 mM HEPES (HyClone), 2 mM L-glutamine (HyClone), 1 mM sodium pyruvate (HyClone), 50 μM β-mercaptoethanol (Sigma-Aldrich), 10% FBS (Gibco), 100 units/ml streptomycin, and 100 units/ml penicillin (HyClone) (complete medium). The cells were seeded (13,000 cells/well) in 96-well plates (Nunc) that had been precoated with fibronectin (Sigma-Aldrich; 5 μg/ml in PBS) for 1 h at 37 °C and subsequently washed three times with PBS. Approximately 2 days after the cells were plated and had grown to ~70% confluency, they were washed three times with PBS and fresh RPMI 1640 medium lacking supplements was added. The cells were then challenged by 22 h of incubation with serum free RPMI containing 102 μM monomeric IAPP, added alone or together with either C4BP (0.15–0.6 μM), transthyretin (5.5 μM, negative control), human IgG (2 μM, negative control), or recombinant DAF (2 μM, negative control). Cell medium with DMSO alone (1%) was used as control. After 22 h, the cells were photographed using an EVOS XL-core microscope (Life Technologies), and the medium was aspirated and replaced with 135 μl of fresh complete RPMI 1640 medium and 15 μl of alamarBlue (Invitrogen) per well. After incubation at 37 °C for ~8 h, the plate was analyzed using spectrophotometer (Cary 50) at 570 and 600 nm. The cell viability in each well was estimated by subtracting absorbance value at 600 nm from the corresponding value at 570 nm.

Cell viability was also studied using markers for early apoptosis (Annexin V-APC; ImmunoTools) and late apoptotic/necrotic cells (Via-Probe; BD Bioscience) combined with flow cytometry. The cells were seeded in 48- or 24-well plates (Nunc) at a concentration of 100,000 or 200,000 cells/well, respectively, in the complete medium and grown for 24 h. The cells were washed twice in PBS and samples (250 or 500 μl) containing 102 μM monomeric IAPP with 0.6 μM C4BP or 2 μM human IgG or 2 μM DAF, as well as 0.6 μM C4BP with 1% DMSO and 1% DMSO were prepared in the complete medium without FBS and added to the cells and incubated overnight (14 h). The cells were harvested with trypsin-EDTA (HyClone) and stained with Annexin V-APC (1:25) and Via-Probe (1:10) diluted in binding buffer (10 mM HEPES, pH 7.4, 150 mM NaCl, 5 mM KCl, 1 mM $MgCl_2$, 1.8 mM $CaCl_2$, and 30 mM NaN_3) in a volume of 50 μl and incubated for 15 min at room temperature. The cells were analyzed using the CyFlow Space flow cytometer (Partec), and the results were analyzed with FlowJo software (Tree Star).

Insulin Secretion from INS-1 Cells—The cells were seeded overnight in 96-well plates in complete medium and then incubated overnight in Optimem with 51 μM monomeric IAPP alone or with one of the proteins: 0.6 μM C4BP, 0.6 μM C1q, 2 μM DAF, 2 μM IgG. The cells were then incubated in Krebs-Ringer buffer supplemented with 2.8 or 16.7 mM glucose for 1 h at 37 °C. The cells were lysed with radioimmune precipitation assay buffer (50 mM Tris-HCl, 150 mM NaCl, 1% Nonidet P-40, 0.5% sodium deoxycholate), and protein concentrations were determined with BCA kit (Pierce). Secreted insulin was quantified using ELISA kit (Mercodia) and normalized to total protein concentration.

Internalization of IAPP/C4BP and Staining of Cells with LysoTracker and MitoTracker—INS-1 cells were seeded on ibidi μ-slide $VI^{0.4}$ ibiTreat (ibidi) (30,000 cells/slide) in the complete medium; after 24 h, the cells were incubated for 3 h in 37 °C with 0 or 51 μM monomeric IAPP containing 10% IAPP labeled with Rhodamine B (Caslo) alone or together with 0.6 μM unlabeled C4BP with or without addition of 1% C4BP labeled with AF647 in complete medium without FBS. LysoTracker Green DND-26 (Molecular Probes) was diluted in prewarmed complete medium to 75 nM and added to the cells for 30 min, and the solution was then replaced with medium containing 200 nM MitoTracker Deep Red FM (Molecular Probes) and 75 nM LysoTracker, for another 30 min. After the incubation the medium was replaced with prewarmed (37 °C) colorless DMEM (Gibco) containing 0.1 mM HEPES (Hyclone). The cells were directly analyzed with live cell imaging in confocal microscope (Zeiss LCM 510). All images are representative of at least three independent staining experiments. Co-localization of IAPP and C4BP was calculated using CoLocalizer Pro (CoLocalization Research Software) and 10 representative images (43).

mRNA Expression Microarray—The INS-1 cells were grown as 5 separate clones for 10 passages before plating in a 12-well plate (Nunc) at 100,000 cells/well and grown in complete RPMI 1640 medium to 70% confluency for ~48 h. The cells were then challenged by adding 77 μM monomeric IAPP alone or together with 0.6 μM C4BP. DMSO (1%), as well as 0.6 μM C4BP alone, were used as controls. After 10 h the medium was aspirated, and the cells were stored at −20 °C pending cell lysis, RNA extraction, and purification according to Qiagen RNeasy kit protocol. The quality of purified RNA was evaluated with both Nanodrop measurement of 230/260 ratios and analysis with Experion RNA-analysis (Bio-Rad). The microarray analysis was carried out on a Rat Gene-2.0 array chip (Affymetrix) by SciBlu Genomics (Lund University).

Data analysis was carried out using R and Bioconductor. The raw data were summarized and normalized using the Robust Multi Average algorithm (21) in which raw intensities are background-corrected, log2-transformed, and quantile-normalized. Normalized data were found to be of excellent quality with sample to sample correlations >0.98 and normalized unscaled standard errors close to 1. To identify differentially expressed genes, a linear model was fitted to the normalized data using the limma package (22), and genes with an FDR-corrected p value < 0.05 were considered differentially expressed. The resulting gene list was functionally characterized using IPA (Ingenuity® Systems) and GOrilla (23). Pathways were visualized using the R-package Pathview. The microarray data were deposited in the Gene Expression Omnibus database with accession number GSE79224.

Cell Viability Assay after Cholesterol Depletion and Filipin III Staining—For depletion of cholesterol from INS-1 cell membranes, two cholesterol-depleting agents MβCD (Sigma-Al-

drich) and CHOD (Sigma-Aldrich) were used. The cells were seeded 30,000 cells in ibidi μ-slide VI$^{0.4}$ ibiTreat chamber and incubated overnight. The media in the chambers were replaced with colorless DMEM (Gibco) containing 0.1 mM HEPES and in half of the chambers supplemented with 2 mM MβCD for 1 h at 37 °C. Thereafter, the solution in the chambers was replaced with complete medium (no FBS) with 0.5% DMSO, 51 μM monomeric IAPP, or 51 μM monomeric IAPP, and 0.3 μM C4BP. Half of the samples contained 2 mM MβCD and were added to the cells that already have been pretreated with MβCD, and the other half of the samples containing no cholesterol-depleting agent were added to untreated cells. INS-1 cells were also treated with 0.5 unit/ml CHOD dissolved in potassium phosphate buffer (pH 7.2) and further diluted in complete medium without FBS alone or together with 51 μM monomeric IAPP or 51 μM monomeric IAPP and 0.3 μM C4BP. Half of the samples were treated with CHOD, and the other half were left untreated. After 14 h of incubation at 37 °C, the chambers were washed three times with PBS, and the cells were fixed for 30 min in room temperature with 4% BD CellFIX diluted in PBS. The cells were washed three times with PBS and then incubated with 1.5 mg/ml glycine for 15 min at room temperature. After another washing cycle, the cells were incubated with 50 μg/ml Filipin III from *Streptomyces filipinensis* (Filipin III; Sigma-Aldrich) diluted in PBS for 30 min at room temperature. After washing with PBS, fluorescence mounting medium (Dako) was added, and the cells were analyzed using confocal microscopy with two-photon laser (Zeiss LCM 510) and Zen software for quantification of the fluorescent intensity.

For assessment of cell viability, INS-1 cells (250,000 cells/well) were seeded in a 24-well plate (Nunc) and pretreated with MβCD as described above. Samples containing 2 mM MβCD or 0.5 unit/ml CHOD in colorless DMEM (Gibco) with 0.1 mM HEPES were supplemented with 0.5% DMSO, 51 μM monomeric IAPP, or 51 μM monomeric IAPP and 0.3 μM C4BP. The cells were incubated overnight and stained with Annexin V-APC and Via-Probe as described above.

Cell Viability Assay for INS-1 Cells Treated with Signaling Pathway Inhibitors—The signaling inhibitors Ly29402 hydrochloride (PI3K inhibitor; Sigma-Aldrich) and BAY112085 (NF-κB inhibitor; Sigma-Aldrich) were diluted in complete medium without FBS to final concentrations of 20 and 2 μM, respectively. The medium also contained 51 μM monomeric IAPP alone or with 0.3 μM C4BP. The cells were incubated for 20 h and after that harvested with trypsin and stained with Annexin V-APC and Via-Probe as described above.

Author Contributions—J S. performed the experiments presented in Figs. 1 and 2 (*A*–*G*) and prepared mRNA for microarray analysis. E. B. and S. C. N. performed the experiments presented in Figs. 2 (*H* and *I*), 4, and 6. K. K. performed the experiments in Figs. 2 (*J* and *K*) and 3*B*. U. K. contributed the experiment in Fig. 3*A*, as well as bioinformatic analyses. E. Z. contributed to the experiments using confocal microscopy. P. S. performed analyses of the microarray data. A. M. B. together with B. C. K., E. R., and G. T. W. conceived the idea for the project, provided crucial reagents, and protocols and wrote the paper. All authors read the manuscript and introduced improvements.

Acknowledgments—We are grateful for expert technical help of Britt-Marie Nilsson and for valuable comments from Prof. Sara Linse (Lund University).

References

1. Blom, A. M., Villoutreix, B. O., and Dahlbäck, B. (2004) Functions of human complement inhibitor C4b-binding protein in relation to its structure. *Arch. Immunol. Ther. Exp.* (*Warsz.*) **52,** 83–95
2. Ricklin, D., Hajishengallis, G., Yang, K., and Lambris, J. D. (2010) Complement: a key system for immune surveillance and homeostasis. *Nat. Immunol.* **11,** 785–797
3. Hillarp, A., and Dahlbäck, B. (1990) Cloning of cDNA coding for the β chain of human complement component C4b-binding protein: sequence homology with the α chain. *Proc. Natl. Acad. Sci. U.S.A.* **87,** 1183–1187
4. Trouw, L. A., Bengtsson, A. A., Gelderman, K. A., Dahlbäck, B., Sturfelt, G., and Blom, A. M. (2007) C4b-binding protein and factor H compensate for the loss of membrane-bound complement inhibitors to protect apoptotic cells against excessive complement attack. *J. Biol. Chem.* **282,** 28540–28548
5. Trouw, L. A., Nilsson, S. C., Gonçalves, I., Landberg, G., and Blom, A. M. (2005) C4b-binding protein binds to necrotic cells and DNA, limiting DNA release and inhibiting complement activation. *J. Exp. Med.* **201,** 1937–1948
6. Blom, A. M., Hallström, T., and Riesbeck, K. (2009) Complement evasion strategies of pathogens-acquisition of inhibitors and beyond. *Mol. Immunol.* **46,** 2808–2817
7. Olivar, R., Luque, A., Naranjo-Gómez, M., Quer, J., García de Frutos, P., Borràs, F. E., Rodríguez de Córdoba, S., Blom, A. M., and Aran, J. M. (2013) The α7β0 isoform of the complement regulator C4b-binding protein induces a semimature, anti-inflammatory state in dendritic cells. *J. Immunol.* **190,** 2857–2872
8. Blom, A. M., Bergström, F., Edey, M., Diaz-Torres, M., Kavanagh, D., Lampe, A., Goodship, J. A., Strain, L., Moghal, N., McHugh, M., Inward, C., Tomson, C., Frémeaux-Bacchi, V., Villoutreix, B. O., and Goodship, T. H. (2008) A novel non-synonymous polymorphism (p.Arg240His) in C4b-binding protein is associated with atypical hemolytic uremic syndrome and leads to impaired alternative pathway cofactor activity. *J. Immunol.* **180,** 6385–6391
9. Mohlin, F. C., Mercier, E., Fremeaux-Bacchi, V., Liszewski, M. K., Atkinson, J. P., Gris, J. C., and Blom, A. M. (2013) Analysis of genes coding for CD46, CD55, and C4b-binding protein in patients with idiopathic, recurrent, spontaneous pregnancy loss. *Eur. J. Immunol.* **43,** 1617–1629
10. Trouw, L. A., Nielsen, H. M., Minthon, L., Londos, E., Landberg, G., Veerhuis, R., Janciauskiene, S., and Blom, A. M. (2008) C4b-binding protein in Alzheimer's disease: Binding to Aβ(1–42) and to dead cells. *Mol. Immunol.* **45,** 3649–3660
11. Sjöberg, A. P., Nyström, S., Hammarström, P., and Blom, A. M. (2008) Native, amyloid fibrils and β-oligomers of the C-terminal domain of human prion protein display differential activation of complement and bind C1q, factor H and C4b-binding protein directly. *Mol. Immunol.* **45,** 3213–3221
12. Sjölander, J., Westermark, G. T., Renström, E., and Blom, A. M. (2012) Islet amyloid polypeptide triggers limited complement activation and binds complement inhibitor C4b-binding protein, which enhances fibril formation. *J. Biol. Chem.* **287,** 10824–10833
13. Jurgens, C. A., Toukatly, M. N., Fligner, C. L., Udayasankar, J., Subramanian, S. L., Zraika, S., Aston-Mourney, K., Carr, D. B., Westermark, P., Westermark, G. T., Kahn, S. E., and Hull, R. L. (2011) β-Cell loss and β-cell apoptosis in human type 2 diabetes are related to islet amyloid deposition. *Am. J. Pathol.* **178,** 2632–2640
14. Kahn, S. E., D'Alessio, D. A., Schwartz, M. W., Fujimoto, W. Y., Ensinck, J. W., Taborsky, G. J., Jr, and Porte, D., Jr. (1990) Evidence of cosecretion of islet amyloid polypeptide and insulin by β-cells. *Diabetes* **39,** 634–638
15. Cavaghan, M. K., Ehrmann, D. A., and Polonsky, K. S. (2000) Interactions between insulin resistance and insulin secretion in the development of glucose intolerance. *J. Clin. Invest.* **106,** 329–333

16. Haataja, L., Gurlo, T., Huang, C. J., and Butler, P. C. (2008) Islet amyloid in type 2 diabetes, and the toxic oligomer hypothesis. *Endocr. Rev.* **29,** 303–316
17. Engel, M. F., Khemtémourian, L., Kleijer, C. C., Meeldijk, H. J., Jacobs, J., Verkleij, A. J., de Kruijff, B., Killian, J. A., and Höppener, J. W. (2008) Membrane damage by human islet amyloid polypeptide through fibril growth at the membrane. *Proc. Natl. Acad. Sci. U.S.A.* **105,** 6033–6038
18. Ritzel, R. A., Meier, J. J., Lin, C. Y., Veldhuis, J. D., and Butler, P. C. (2007) Human islet amyloid polypeptide oligomers disrupt cell coupling, induce apoptosis, and impair insulin secretion in isolated human islets. *Diabetes* **56,** 65–71
19. Paulsson, J. F., Schultz, S. W., Köhler, M., Leibiger, I., Berggren, P. O., and Westermark, G. T. (2008) Real-time monitoring of apoptosis by caspase-3-like protease induced FRET reduction triggered by amyloid aggregation. *Exp. Diabetes Res.* **2008,** 865850
20. Trikha, S., and Jeremic, A. M. (2011) Clustering and internalization of toxic amylin oligomers in pancreatic cells require plasma membrane cholesterol. *J. Biol. Chem.* **286,** 36086–36097
21. Caillon, L., Hoffmann, A. R., Botz, A., and Khemtemourian, L. (2016) Molecular structure, membrane interactions, and toxicity of the islet amyloid polypeptide in type 2 diabetes mellitus. *J. Diabetes Res.* **2016,** 5639875
22. Janson, J., Ashley, R. H., Harrison, D., McIntyre, S., and Butler, P. C. (1999) The mechanism of islet amyloid polypeptide toxicity is membrane disruption by intermediate-sized toxic amyloid particles. *Diabetes* **48,** 491–498
23. Knight, J. D., and Miranker, A. D. (2004) Phospholipid catalysis of diabetic amyloid assembly. *J. Mol. Biol.* **341,** 1175–1187
24. Lopes, D. H., Meister, A., Gohlke, A., Hauser, A., Blume, A., and Winter, R. (2007) Mechanism of islet amyloid polypeptide fibrillation at lipid interfaces studied by infrared reflection absorption spectroscopy. *Biophys. J.* **93,** 3132–3141
25. Blom, A. M., Webb, J., Villoutreix, B. O., and Dahlbäck, B. (1999) A cluster of positively charged amino acids in the N-terminal modules of the C4BP a-chain is crucial for C4b binding and factor I cofactor function. *J. Biol. Chem.* **274,** 19237–19245
26. Spijkers, P. P., Denis, C. V., Blom, A. M., and Lenting, P. J. (2008) Cellular uptake of C4b-binding protein is mediated by heparan sulfate proteoglycans and CD91/LDL receptor-related protein. *Eur. J. Immunol.* **38,** 809–817
27. Oskarsson, M. E., Singh, K., Wang, J., Vlodavsky, I., Li, J. P., and Westermark, G. T. (2015) Heparan sulfate proteoglycans are important for islet amyloid formation and islet amyloid polypeptide-induced apoptosis. *J. Biol. Chem.* **290,** 15121–15132
28. Negi, S., Jetha, A., Aikin, R., Hasilo, C., Sladek, R., and Paraskevas, S. (2012) Analysis of beta-cell gene expression reveals inflammatory signaling and evidence of dedifferentiation following human islet isolation and culture. *PLoS One* **7,** e30415
29. Masters, S. L., Dunne, A., Subramanian, S. L., Hull, R. L., Tannahill, G. M., Sharp, F. A., Becker, C., Franchi, L., Yoshihara, E., Chen, Z., Mullooly, N., Mielke, L. A., Harris, J., Coll, R. C., Mills, K. H., *et al.* (2010) Activation of the NLRP3 inflammasome by islet amyloid polypeptide provides a mechanism for enhanced IL-1β in type 2 diabetes. *Nat. Immunol.* **11,** 897–904
30. Magzoub, M., and Miranker, A. D. (2012) Concentration-dependent transitions govern the subcellular localization of islet amyloid polypeptide. *FASEB J.* **26,** 1228–1238
31. Rodal, S. K., Skretting, G., Garred, O., Vilhardt, F., van Deurs, B., and Sandvig, K. (1999) Extraction of cholesterol with methyl-β-cyclodextrin perturbs formation of clathrin-coated endocytic vesicles. *Mol. Biol. Cell* **10,** 961–974
32. Vrielink, A. (2010) Cholesterol oxidase: structure and function. *Subcell. Biochem.* **51,** 137–158
33. Quist, A., Doudevski, I., Lin, H., Azimova, R., Ng, D., Frangione, B., Kagan, B., Ghiso, J., and Lal, R. (2005) Amyloid ion channels: a common structural link for protein-misfolding disease. *Proc. Natl. Acad. Sci. U.S.A.* **102,** 10427–10432
34. Singh, S., Trikha, S., Bhowmick, D. C., Sarkar, A. A., and Jeremic, A. M. (2015) Role of cholesterol and phospholipids in amylin misfolding, aggregation and etiology of islet amyloidosis. *Adv. Exp. Med. Biol.* **855,** 95–116
35. Cho, W. J., Jena, B. P., and Jeremic, A. M. (2008) Nano-scale imaging and dynamics of amylin-membrane interactions and its implication in type II diabetes mellitus. *Methods Cell Biol.* **90,** 267–286
36. Lin, C. Y., Gurlo, T., Haataja, L., Hsueh, W. A., and Butler, P. C. (2005) Activation of peroxisome proliferator-activated receptor-γ by rosiglitazone protects human islet cells against human islet amyloid polypeptide toxicity by a phosphatidylinositol 3′-kinase-dependent pathway. *J. Clin. Endocrinol. Metab.* **90,** 6678–6686
37. Tuttle, R. L., Gill, N. S., Pugh, W., Lee, J. P., Koeberlein, B., Furth, E. E., Polonsky, K. S., Naji, A., and Birnbaum, M. J. (2001) Regulation of pancreatic beta-cell growth and survival by the serine/threonine protein kinase Akt1/PKBα. *Nat. Med.* **7,** 1133–1137
38. Dahlbäck, B., and Hildebrand, B. (1983) Degradation of human complement component C4b in the presence of the C4b-binding protein-protein S complex. *Biochem. J.* **209,** 857–863
39. Tenner, A. J., Lesavre, P. H., and Cooper, N. R. (1981) Purification and radiolabeling of human C1q. *J. Immunol.* **127,** 648–653
40. Blom, A. M., Kask, L., and Dahlbäck, B. (2001) Structural requirements for the complement regulatory activities of C4BP. *J. Biol. Chem.* **276,** 27136–27144
41. Jusko, M., Potempa, J., Kantyka, T., Bielecka, E., Miller, H. K., Kalinska, M., Dubin, G., Garred, P., Shaw, L. N., and Blom, A. M. (2014) Staphylococcal proteases aid in evasion of the human complement system. *J. Innate Immun.* **6,** 31–46
42. Hohmeier, H. E., Mulder, H., Chen, G., Henkel-Rieger, R., Prentki, M., and Newgard, C. B. (2000) Isolation of INS-1-derived cell lines with robust ATP-sensitive K^+ channel-dependent and -independent glucose-stimulated insulin secretion. *Diabetes* **49,** 424–430
43. Manders, E. M., Stap, J., Brakenhoff, G. J., van Driel, R., and Aten, J. A. (1992) Dynamics of three-dimensional replication patterns during the S-phase, analysed by double labelling of DNA and confocal microscopy. *J. Cell Sci.* **103,** 857–862